RESEARCH REPORT

EJN European Journal of Neuroscience FENS WILEY

Cholesterol-recognition motifs in the transmembrane domain of the tyrosine kinase receptor family: The case of TRKB

Cecilia Cannarozzo[1] [iD] | Senem Merve Fred[1] [iD] | Mykhailo Girych[2] [iD] |
Caroline Biojone[1] [iD] | Giray Enkavi[2] [iD] | Tomasz Róg[2] [iD] | Ilpo Vattulainen[2,3] [iD] |
Plinio C Casarotto[1] [iD] | Eero Castrén[1] [iD]

[1]Neuroscience Center - HiLife, University of Helsinki, Helsinki, Finland

[2]Department of Physics, University of Helsinki, Helsinki, Finland

[3]Computational Physics Laboratory, Tampere University, Tampere, Finland

Correspondence
Plinio Cabrera Casarotto, Neuroscience Center, Haartmaninkatu 8, B233b. PO Box 63, University of Helsinki, Finland.
Email: plinio.casarotto@helsinki.fi

Funding information
H2020 European Research Council, Grant/Award Number: 322742; Academy of Finland, Grant/Award Number: 294710 and 307416; EU Joint Programme - Neurodegenerative Disease Research, Grant/Award Number: 301225 and 643417

Abstract

Cholesterol is an essential constituent of cell membranes. The discovery of cholesterol-recognition amino acid consensus (CRAC) motif in proteins indicated a putative direct, non-covalent interaction between cholesterol and proteins. In the present study, we evaluated the presence of a CRAC motif and its inverted version (CARC) in the transmembrane region (TMR) of the tyrosine kinase receptor family (RTK) in several species using in silico methods. CRAC motifs were found across all species analyzed, while CARC was found only in vertebrates. The tropomyosin-related kinase B (TRKB), a member of the RTK family, through interaction with its endogenous ligand brain-derived neurotrophic factor (BDNF) is a core participant in the neuronal plasticity process and exhibits a CARC motif in its TMR. Upon identifying the conserved CARC motif in the TRKB, we performed molecular dynamics simulations of the mouse TRKB.TMR. The simulations indicated that cholesterol interaction with the TRKB CARC motif occurs mainly at the central Y433 residue. Our binding assay suggested a bell-shaped effect of cholesterol on BDNF interaction with TRKB receptors, and our results suggest that CARC/CRAC motifs may play a role in the function of the RTK family TMR.

KEYWORDS

BDNF, cholesterol-recognition motif, TRKB, tyrosine kinase family

1 | INTRODUCTION

The human brain contains 23% of the body's total cholesterol. Most of this cholesterol is found in the myelin sheath of oligodendrocytes (Dietschy & Turley, 2004; Martin et al., 2014). As the blood-brain barrier prevents lipoprotein or cholesterol transport to the brain, local de novo synthesis takes place. In the mouse brain, cholesterol synthesis peaks during the second postnatal week and then decreases significantly independent of sex or blood cholesterol concentration (Pfrieger & Ungerer, 2011; Quan et al., 2003). During early development, neurons produce cholesterol autonomously (de Chaves et al., 1997; Nieweg et al., 2009; Pfrieger & Ungerer, 2011). In later stages, cholesterol is synthesized by glial cells. However, it is unknown if this synthesis is constant or under regulated production (Pfrieger & Ungerer, 2011; Saito et al., 2009).

Edited by: Dr. Paola Bovolenta

Cholesterol can be localized on both leaflets of the plasma membrane (Fantini et al., 2016) and induces changes in physical properties of the membrane, such as fluidity (Maguire & Druse, 1989) and curvature (Lee, 2004). Cholesterol can also interact with transmembrane domains to regulate protein function (Elkins et al., 2018; Fantini & Barrantes, 2013). Cholesterol is a core constituent of microdomains known as lipid rafts, which serve as signaling platforms for several pathways (Lang et al., 2001; Pereira & Chao, 2007; Zonta & Minichiello, 2013). In the nervous system, cholesterol interaction with membrane proteins influences several crucial events, such as exocytosis of synaptic vesicles (Linetti et al., 2010), synaptic activity, connectivity, plasticity, signal transduction, transmission, and cell survival (Goritz et al., 2005; Liu et al., 2010; Michikawa & Yanagisawa, 1999).

The tropomyosin-related kinase receptor (TRK) subfamily is one of the most prominent subfamilies of tyrosine kinase receptors (RTK) and plays a crucial role in neuronal plasticity (Dekkers et al., 2013). The TRK receptors consist of three members (TRKA, TRKB, and TRKC, or NTRK1, NTRK2 and NTRK3, respectively), which are phosphorylated on several tyrosine residues on the intracellular portion upon activation by their high-affinity ligands (NGF, BDNF, and NT-3, respectively) (Huang & Reichardt, 2001). TRKA and TRKC are located in lipid rafts, while the transit of TRKB to rafts occurs transiently upon BDNF stimulation (Suzuki et al., 2004, 2007). Functionally, in the absence of ligand, TRKA and TRKC, but not TRKB, induce cell death mediated by interaction with p75NTR, the low-affinity receptor of several neurotrophins (Dekkers et al., 2013; Nikoletopoulou et al., 2010).

In silico models suggest that two cholesterol molecules can interact in a tail-to-tail fashion as a transbilayer dimer (Harris et al., 1995; Rukmini et al., 2001) or back-to-back through their flat alpha faces, leaving the beta sides accessible for interactions with proteins (Hanson et al., 2008). On these target proteins, the following two consensus motifs with predictive value have been defined (Di Scala et al., 2017): the Cholesterol-Recognition Amino acid Consensus sequence (CRAC) and its "inverted" version (CARC) (Baier et al., 2011; Li & Papadopoulos, 1998). The CRAC sequence, from N- to C-terminus, consists of an apolar residue (leucine [L] or valine [V]), one to five amino acids of any kind, an aromatic amino acid (tyrosine [Y] or phenylalanine [F]), one to five amino acids of any kind, and a basic residue (arginine [R] or lysine [K]) (Fantini & Barrantes, 2013). CARC consists of the same pattern in the opposite direction, with tryptophan (W) as an alternative aromatic residue. CARC has a higher affinity for cholesterol than CRAC (Di Scala et al., 2017; Fantini & Barrantes, 2013). Several proteins have been identified to contain CRAC/CARC motifs, such as nicotinic acetylcholine, type-3 somatostatin, and γ-amino-butyric acid receptors (Epand, 2006; Fantini & Barrantes, 2013; Jamin et al., 2005).

We recently identified a CARC domain in TRKB and showed that its mutation interferes with plasticity-related BDNF signaling (Casarotto et al., 2021). The aim of the present study is to evaluate the incidence of cholesterol-interacting motifs (CRAC and CARC) in the RTK family. Given the promiscuous nature of CRAC motifs, we focused on the RTK transmembrane region (TMR; transmembrane domain plus the 5-amino acid flanking residues on both N- and C-terminal sides), where direct interaction with cholesterol is more likely. Transmembrane domains are crucial for proper positioning of proteins in biological membranes (Fantini & Barrantes, 2013). Interaction of the bilayer lipids with the transmembrane domains of embedded integral protein provides a diffusion barrier and seals any gaps in the membrane to maintain electrochemical properties (Hunte, 2005). Upon identification of CRAC/CARC motifs in the TMR of many members of the RTK family, we focused on TRKB and assessed its sequence identity across species. We then investigated the interaction of this motif with cholesterol using molecular dynamic simulations. Then, we expanded our previous findings about the mechanisms behind the cholesterol effect on BDNF-induced TRKB activity (Casarotto et al., 2021) by assaying the binding of biotinylated BDNF to immobilized TRKB.

2 | METHODS

2.1 | Data mining

For data mining, we used 144 manually curated inputs of the RTK family (code 2.7.10.1) from the UniProt database (The UniProt Consortium, 2017). The canonical primary structure of TMR (transmembrane domain and the flanking 5 amino acid residues, from N- and C-terminal) of RTK from each target of human (52 proteins), mouse (51 proteins), zebrafish (14 proteins), fruit fly (12 proteins), and the nematode *C. elegans* (15 proteins) databases were extracted. The TMR FASTA sequences, consisting of the transmembrane domain (TMD) with five flanking amino acid sequences in each side, for each protein were manually screened for the presence of cholesterol-recognition alignment consensus, CRAC and CARC (Fantini & Barrantes, 2013; Fantini et al., 2016). We then searched for putative pathogenic mutations in human proteins using SwissVar, ClinVar, and COSMIC databases (Landrum et al., 2018; Mottaz et al., 2010; Tate et al., 2019).

2.2 | Percentage of identity (PI) of full length TRKB, and TRKB.TMR across species

The Percentage Identity (PI) of TRKB.TMR among several species, including *D. rerio* (zebrafish), *G. gallus* (chicken),

C. familiaris (dog), *R. norvegicus* (rat), *M. musculus* (mouse), *P. troglodytes* (chimpanzee), and *H. sapiens* (human), was determined using the align tool in UniProt database (The UniProt Consortium, 2017). The same comparison was performed independently for full length TRKB from the listed species.

2.3 | Molecular dynamics simulations

The structure of the TMR of TRKB (residues 423–460) was generated using the FMAP (Folding of Membrane-Associated Peptides) server (Lomize et al., 2018). The server predicted that the residues V432-A456 form an α-helical transmembrane segment with the remaining sequence being unstructured. This structure was used as an atomistic model for the TRKB. Coarse-grained protein model of the wild-type TRKB was based on this structure. The TMR of TRKB was embedded in a bilayer (512 lipids) composed of 60 mol% (mole percentage) palmitoyl-oleoyl-phosphatidylcholine (POPC) and 40 mol% cholesterol (60:40 POPC:CHOL) using the CHARMM-GUI Martini Maker (Hsu et al., 2017). The system was solvated with 6,038 water beads (approximately 50 water molecules per lipid). Sodium and chloride ions were added to reach 0.15 M salt concentration and to neutralize the system. The system was first equilibrated with the protein backbone atoms restrained. In the production stage, it was simulated for 5 μs through nine independent repeats. The simulations were performed using Gromacs 5.1.4 (Abraham et al., 2015) employing the non-polarizable Martini 2.2 force field for the protein (de Jong et al., 2013) and lipids (Arnarez et al., 2015). The simulations were performed using the "New-RF" parameters (de Jong et al., 2016). For electrostatics, the reaction field method was used with a cutoff of 1.1 nm. Lennard-Jones interactions were cut off at 1.1 nm. The potential shift modifier was applied to non-bonded interactions together with buffered Verlet lists (Páll & Hess, 2013). The equations of motion were integrated using the leap-frog algorithm with a 25-fs time step. The simulations were performed at 310 K in the NpT ensemble at a pressure of 1 bar. The protein, the membrane, and the solvent (water and 0.15 M NaCl) were coupled to separate heat baths with a time constant of 1.0 ps using the V-rescale thermostat (Bussi et al., 2007). Pressure was controlled semi-isotropically using the Parrinello-Rahman barostat (Parrinello & Rahman, 1981) with a time constant of 12 ps and a compressibility of 3×10^{-4} bar^{-1} in the xy-plane (membrane plane). All analyses were performed using the Gromacs software package and in-house scripts, using only the last 4 μs of the simulations. The data presented (Figure 3) is the average occupancy of cholesterol that represents the average number of cholesterol molecules within 0.6 nm of the alpha carbon (MARTINI backbone bead) of residues R427 and Y433, the key residues of CARC motif (Fantini et al., 2016). The occupancy values are produced by dividing the total number of contacts by the number of frames in each trajectory.

2.4 | Cell cultures and BDNF-binding assay

HEK293T cells were transfected to overexpress full-length TRKB (Casarotto et al., 2021). The cells were maintained at 5% CO2, 37°C in Dulbecco's Modified Eagle's Medium (DMEM, containing 10% fetal calf serum, 1% penicillin/streptomycin, 1% L-glutamine). The cells were lysed, and the lysate was submitted to the BDNF-binding assay.

The BDNF binding to TRKB was performed in white 96-well plates (Baeza-Raja et al., 2016; Casarotto et al., 2021; Das et al., 2015). Briefly, the plates were precoated with anti-TRKB antibody (1:1,000, R&D Systems, #AF1494) in carbonate buffer (pH 9.8) overnight at 4°C, followed by blocking with 3% BSA in PBS buffer (2 hr at RT). The samples (120 μg of total protein) were added and incubated overnight at 4°C under agitation. The plates were washed 3× with PBS buffer, and a mixture of biotinylated BDNF (bBDNF: 0, 0.05, 0.1, 0.5, 1, 5, or 10 ng/ml, Alomone Labs, #B-250-B) and cholesterol (0, 20, 50 or 100 μM) was added for 1h at room temperature, followed by washing with PBS. A competitive assay was performed with a mixture of bBDNF (1 ng/ml) and non-biotinylated BDNF (0, 0.05, 0.1, 0.5, 1, 5, 10, or 20 ng/ml, Peprotech, #450-02). The luminescence was determined via HRP-conjugated streptavidin (1:10,000, 1h, RT, Thermo-Fisher, #21126) activity reaction with ECL by a plate reader. The luminescence signal from blank wells (containing all the reagents but the sample lystates, substituted by the blocking buffer) was used as background. The specific signal was then calculated by subtracting the values of blank wells from the values of the samples with matched concentration of the biotinylated ligand. The signal was normalized by the bBDNF at 10 ng/ml under no added cholesterol (0 μM).

2.5 | Statistical analysis

The correlation between PI in full-length TRKB and TRKB.TMR among the different species was determined by Spearman's test. The PI trees for full TRKB and TMR. TRKB were obtained using the tree tool (Neighbour Joining, BLOSUM62) in Jalview v.2.0 software (Waterhouse et al., 2009). The data from MD simulations were analyzed by Student *t* test, and the results from bBDNF-binding assay were analyzed by two-way ANOVA. Non-linear regression curve fitting (One-site specific binding for bBDNF alone, and One-site - fit Ki for competition assay) was used to derive dissociation constant (Kd) and maximum binding (Bmax) using GraphPad Prism v.6.07. $p < .05$ were considered significant.

3 | RESULTS

3.1 | Data mining

The presence of CRAC motifs within the TMDs of RTK family members was found throughout all the species analyzed (human, 11 of 52 proteins; mouse, 10 of 51 proteins; zebrafish, 2 of 14 proteins; fruit fly, 2 of 12 proteins; and C. elegans, 2 of 15 proteins, Figure 1). However, the presence of CARC motifs in the RTK family was observed only in vertebrates, with 3 in human, 3 in mouse, and 2 in zebrafish RTK. None of the proteins analyzed was found to carry CRAC and CARC motifs simultaneously. The ClinVar and COSMIC databases indicated eight mutations in the CRAC/CARC motifs of five proteins (Table 1) associated with central nervous system or endocrine disorders, or cancer.

The full list of proteins positive to CRAC/CARC is found in Table 1 and the full list of proteins examined from each species can be found in the deposited data.

3.2 | Percentage of identity (PI) of full length TRKB, and TRKB.TMR across species

We previously found that TRKB is the only member of the TRK-subfamily of RTKs that possesses a CARC domain (Casarotto et al., 2021). The CARC motif in TRKB was conserved across species: human and mouse, REHLSVYAVVV;

zebrafish, RVAVYIVV. It has been previously pointed out that the TMR of TRKB is functionally distinct from that of other TRK family members (Dekkers et al., 2013; Nikoletopoulou et al., 2010). We therefore examined the identity between TRKB.TMR sequences of several species (human, chimpanzee, mouse, rat, dog, chicken, and zebrafish; Table 2) using UniProt (The UniProt Consortium, 2017). Over 90% PI was found in TRKB.TMR, as well as in full-length TRKB of human, chimpanzee, mouse, rat, and dog. The PI results of paired comparisons of TRKB.TMR sequences between the species analyzed are organized in Figure 2. For comparison, we also determined the PI of full-length TRKB among these species. The PI results of paired comparisons are also organized in Figure 2, and Spearman's test indicated a significant correlation between the PI in full-length TRKB and TRKB. TMR [R^2 = 0.8530, 99% confidence interval, CI = 0.8135–0.9698; p < .0001].

3.3 | Molecular dynamics simulations

To study the interaction between cholesterol and TRKB. TMR, we performed coarse-grained molecular dynamics simulations with a single TMR embedded in a 60:40 (mol%) POPC:CHOL bilayer. Representative interaction modes between TRKB.TMR and cholesterol are shown in Figure 3a,b and in the supplemental movie. Analysis of the trajectories
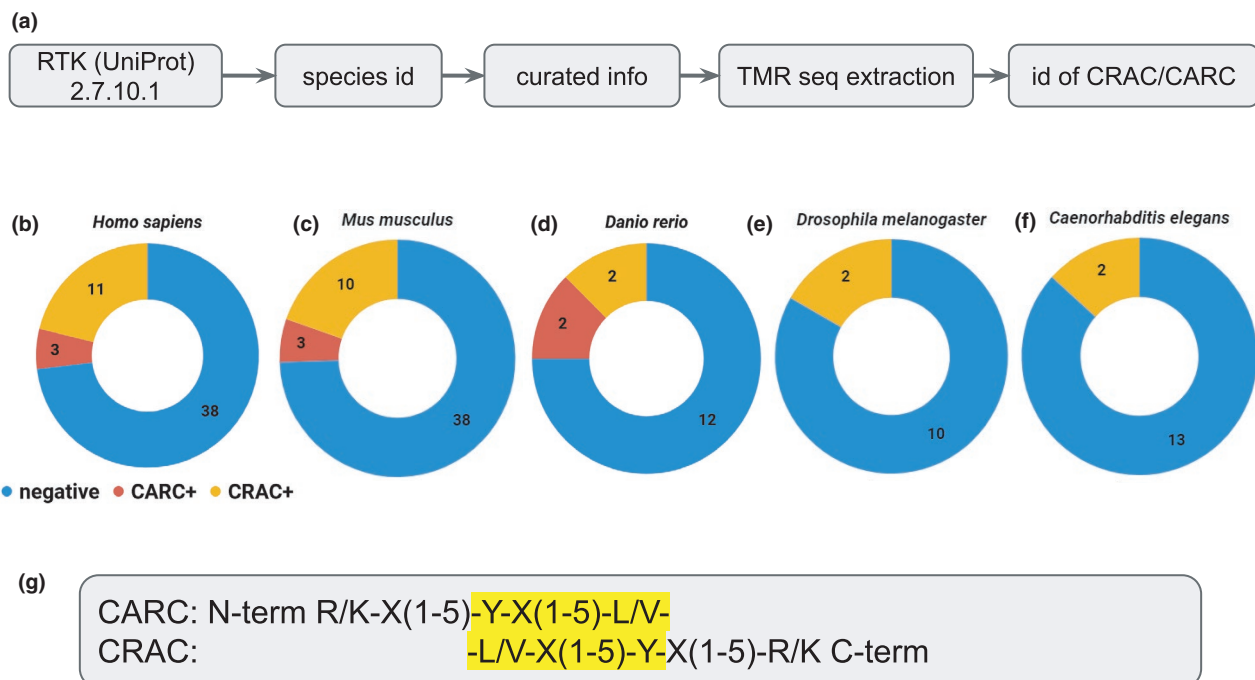
FIGURE 1 (a) Workflow of data mining. The TMR (transmembrane sequence +5 amino acid residues from each N- and C-terminal sides) of curated entries found in UniProt using the code for tyrosine-kinase receptor family (2.7.10.1) were screened for the presence of cholesterol recognition and alignment consensus (CRAC and CARC). The incidence of CRAC and CARC motifs in (b) human, (c) mouse, (d) zebrafish, (e) fruit fly, and (f) *C. elegans* TMR of RTK family members. (g) Library of CRAC and CARC sequences (all combinations used can be found in the stored data). Residue sequence predicted to be embedded into the cell membrane shown in yellow

TABLE 1 CRAC and CARC(underlined)-positive proteins in the transmembrane region

Unipro ID	Protein name	Mutation in CRAC/CARC
H. sapiens		
Q9UM73	ALK tyrosine kinase receptor	
Q16620	BDNF/NT−3 growth factors receptor	Y434C
P29320	Ephrin type-A receptor 3	I564V
P11362	Fibroblast growth factor receptor 1	
P22455	Fibroblast growth factor receptor 4	
P08069	Insulin-like growth factor 1 receptor	
P06213	Insulin receptor	F978Y
P07333	Macrophage colony-stimulating factor 1 receptor	L536V, Y540S, K541T, K543 M
P10721	Mast/stem cell growth factor receptor Kit	
O15146	Muscle, skeletal receptor tyrosine-protein kinase	
Q15303	Receptor tyrosine-protein kinase erbB−4	
Q12866	Tyrosine-protein kinase Mer	I518V
Q01974	Tyrosine-protein kinase receptor ROR2	
P34925	Tyrosine-protein kinase RYK	
M. musculus		
P97793	ALK tyrosine kinase receptor	
P15209	BDNF/NT−3 growth factors receptor	
Q60750	Ephrin type-A receptor 1	
P29319	Ephrin type-A receptor 3	
P16092	Fibroblast growth factor receptor 1	
Q03142	Fibroblast growth factor receptor 4	
P15208	Insulin receptor	
Q60751	Insulin-like growth factor 1 receptor	
P09581	Macrophage colony-stimulating factor 1 receptor	
P05532	Mast/stem cell growth factor receptor Kit	
Q61006	Muscle, skeletal receptor tyrosine-protein kinase	

(Continues)

TABLE 1 (Continued)

Unipro ID	Protein name	Mutation in CRAC/CARC
Q9Z138	Tyrosine-protein kinase transmembrane receptor ROR2	
Q01887	Tyrosine-protein kinase RYK	
D. rerio		
Q9I8N6	Macrophage colony-stimulating factor 1 receptor	
Q8JFR5	Mast/stem cell growth factor receptor kita	
B8JLJ1	Tyrosine-protein kinase receptor (Ntrk2a)	
A0A0R4ILA2	Tyrosine-protein kinase receptor (Ntrk2b)	
D. melanogaster		
P09208	Insulin-like receptor	
P83097	Putative tyrosine-protein kinase Wsck	
C. elegans		
P34891	Receptor-like tyrosine-protein kinase kin−15	
G5EGK5	Tyrosine-protein kinase receptor cam−1	

in terms of average cholesterol occupancy (see Methods) revealed that cholesterol has higher occupancy close to Y433 compared to R427, showing a preference for the aromatic residue of TRKB CARC domain [$t(16) = 62.46$, $p < .0001$], as shown in Figure 3c.

3.4 | BDNF-binding assay

As shown in Figure 3d, the binding of bBDNF to immobilized TRKB is altered by the concentration of cholesterol added to the samples. We found that moderate concentrations of added cholesterol (20 µM) facilitate bBDNF binding to TRKB, while higher amounts of cholesterol (50 or 100 µM) compromise bBDNF interaction with immobilized TRKB (Figure 3d). The two-way ANOVA indicated an interaction between cholesterol and BDNF binding [$F(18,140) = 4.155$, $p < .0001$]. Scatchard analysis (Figure 3d, insert) indicates that the effects of cholesterol are mostly produced by differences in available bBDNF-binding sites (for Bmax and Kd values for each condition, please see the legend for Figure 3). A bell-shaped effect of cholesterol on BDNF binding to TRKB is further evidenced by the curve for bBDNF at 1 ng/ml under different concentrations of cholesterol (Figure 3e, [interaction: $F(3,40) = 11.50$, $p < .0001$]). We and others

UniProt	Species	TMR sequence
Q16620	*H. sapiens*	TG[REHLSVYAVVV]IASVVGFCLLVM LFLLKLARH
A0A2J8MRP9	*P. troglodites*	TG[REHLSVYAVVV]IASVVGFCLLVM LFLLKLARH
P15209	*M. musculus*	SN[REHLSVYAVVV]IASVVGFCLLVM LLLLKLARH
Q63604	*R. norvegicus*	TN[REHLSVYAVVV]IASVVGFCLLVM LLLLKLARH
E2RKA1	*C. familiaris*	SG[REHLSVYAVVV]IASVVGFCLLVM LFLLKLARH
Q91987	*G. gallus*	EN[EDSITVYVVV]GIAALVCTGLVIML IILKFGRH
A0A0R4ILA2	*D. rerio*	PLE[DRVAVYIVV]GIAGVALTGCILML VFLKYGRS

T A B L E 2 CARC-containing sequences ([red,brackets]) in the TRKB. TMR among vertebrate species

(a)

TRKB.TMR	human	chimpanzee	mouse	rat	dog	chicken
human						
chimpanzee	100.00					
mouse	91.18	91.18				
rat	94.12	94.12	97.06			
dog	97.06	97.06	94.12	91.18		
chicken	41.18	41.18	44.12	44.12	41.18	
zebrafish	35.29	35.29	35.29	35.29	35.29	50.00

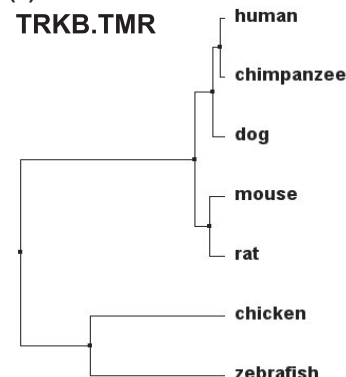| TRKB	human	chimpanzee	mouse	rat	dog	chicken
human						
chimpanzee	100.00					
mouse	93.92	93.92				
rat	93.55	93.55	98.54			
dog	98.30	98.30	93.80	93.55		
chicken	77.13	77.13	76.49	76.49	77.49	
zebrafish	60.43	60.43	60.39	60.15	60.68	61.09
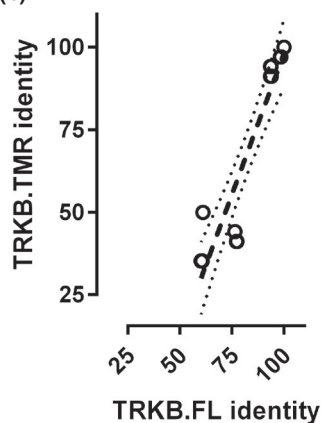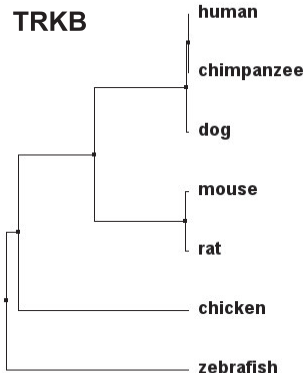
FIGURE 2 (a) Percent identity (PI) for TRKB. TMR (left; sequences for TRKB.TMR found in Table 2) and for TRKB full length (right). The amino acid sequence of TRKB.TMR, and TRKB full length (NTRK2) from different species were verified for PI in the UniProt database. (b) Correlation between the PI of full length TRKB and TMR of TRKB [Spearman's test. $R^2 = 0.8530$; 99%CI = 0.7564 to 0.9775; $p < .0001$]; dashed line = 99% confidence band. PI tree of (c) full length, and (d) TMR of TRKB

have previously shown that reduction of cholesterol levels under those normally present in cultured cells (by cholesterol synthesis inhibitor pravastatin, for example) compromises the effects of BDNF (Casarotto et al., 2021; Suzuki et al., 2004),

further emphasizing the bell-shaped response. As control, the binding of bBDNF (1 ng/ml) to immobilized TRKB was displaced by increasing concentrations of unlabeled BDNF (0, 0.05, 0.1, 0.5, 1, 5, 10, or 20 ng/ml) as seen in Figure 3f.
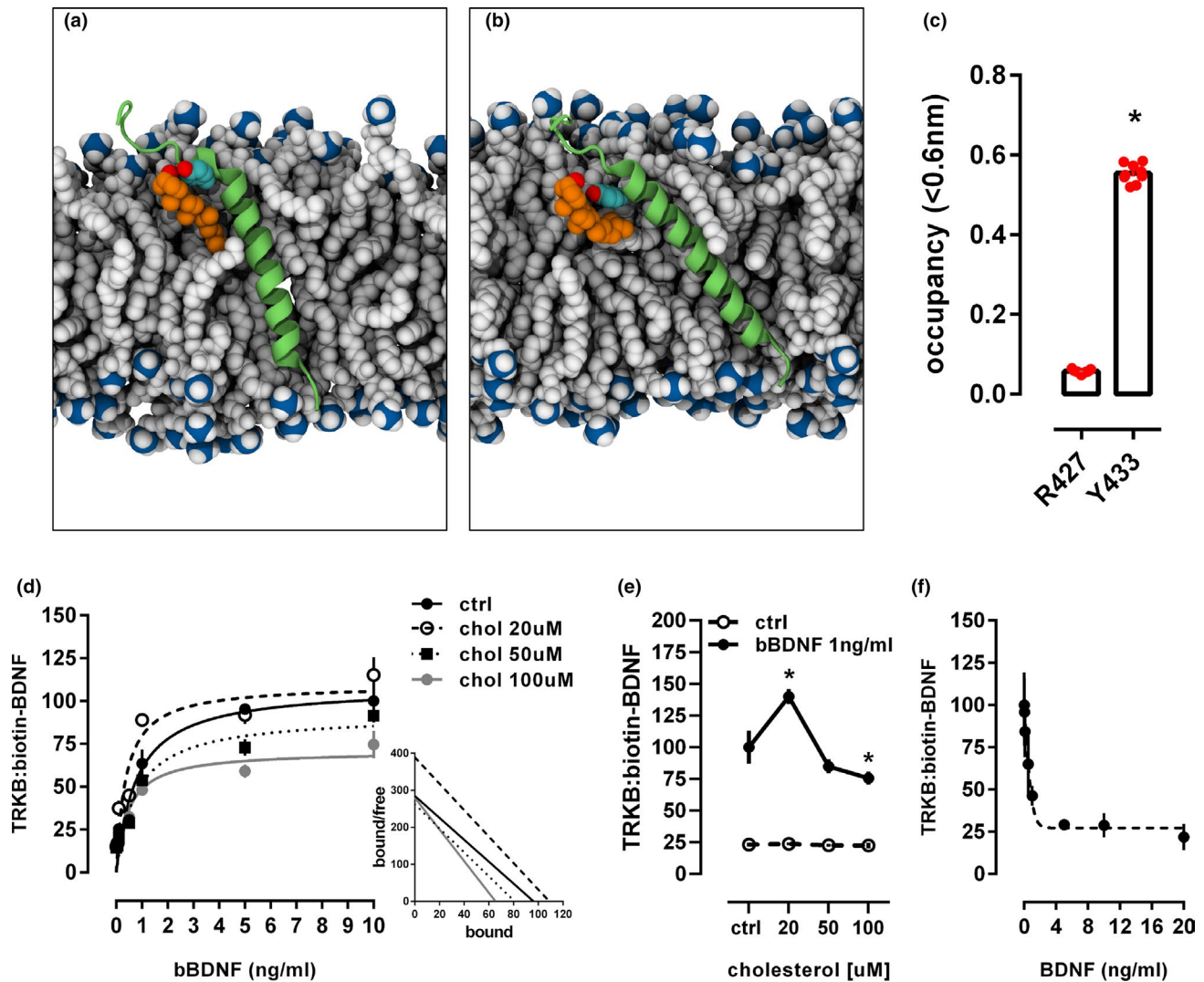
FIGURE 3 TRKB interaction with cholesterol. (a,b) Snapshots of the interaction between TRKB and cholesterol at the TMR (see supplement video) indicating that cholesterol (orange) interacts with the OH- group (red) in Y433 (cyan) of the TRKB.TMR (green). The TRKB.TMR helix is shown in the cartoon, the lipids and Y433 sidechain in van der Waals representations. (c) Molecular dynamics simulations show that cholesterol predominantly resides close to the C-alpha atom of Y433 but not C-alpha atom of R427, highlighting the significance of the aromatic Y in the TRKB CARC domain. (d) The binding of biotinylated BDNF (bBDNF) to TRKB is modulated by added cholesterol in a bell-shaped fashion [from Scatchard analysis Kd for bBDNF ctrl: 2.77 pM; chol 20 μM: 2.27pM; chol 50 μM: 2.61 pM; chol 100 μM: 1.93 pM; Bmax for bBDNF ctrl: 96.18; chol 20 μM: 108.9; chol 50 μM: 80.81; chol 100 μM: 65.35]. Curves from the Scatchard transformation of the TRKB:BDNF binding are depicted in the insert. Data expressed as mean/*SEM* of binding normalized by bBDNF10 ng/ml ctrl (no added cholesterol). (e) Expansion of the binding of bBDNF 1 ng/ml (black circles) and bBDNF 0 (ctrl, open circles), depicting the bell-shaped effect of different concentrations of cholesterol on bBDNF:TRKB interaction. Data expressed as mean/*SEM* of binding normalized by bBDNF 1 ng/ml ctrl. (f) Unlabeled BDNF (0-20 ng/ml) dislocates bBDNF (1 ng/ml) binding to immobilized TRKB assayed at no supplemented cholesterol (0 μM). Data expressed as mean/*SEM* normalized by bBDNF 1 ng/ml at BDNF 0 ng/ml. *$p < .05$ from control (BDNF 1 ng/ml–cholesterol ctrl, R427)

4 | DISCUSSION

In the present study, we evaluated the incidence of cholesterol-recognition motifs in the TMR of the RTK family from mouse, human, zebrafish, fruit fly, and the nematode *C. elegans*. We found that while the bona fide CRAC motif, located in the C-terminal portion of the transmembrane domain (Fantini & Barrantes, 2013), is found in all

species analyzed, its inverted version (CARC) was observed only in vertebrates. Furthermore, we found that TRKB, a tyrosine-kinase receptor crucial for neuronal plasticity, contains in the TMR, a CARC sequence (Casarotto et al., 2021) that is conserved across different species. However, CRAC/CARC motifs were absent in the TMR of other members of the TRK subfamily, such as TRKA and TRKC (Casarotto et al., 2021).

Cholesterol can interact with membrane proteins in several ways. One of its most prominent effects involves a direct post-translational modification on members of the Hedgehog pathway described in *Drosophila sp.* (Jeong & McMahon, 2002; Wendler et al., 2006). In this model organism, cholesterol also regulates membrane depolarization through transient receptor potential (TRP) channels (Peters et al., 2017) and serves as a precursor for ecdysteroids, which in turn control several steps of the fly development (Niwa & Niwa, 2014). In nematodes such as C. elegans, cholesterol is only obtained from diet, although these worms can modify the basic steroid structure into derivatives (Kurzchalia & Ward, 2003). In both organisms, cholesterol appears to play a major role as a signaling molecule with post-translational modifications of proteins as the main mechanism (Mann & Beachy, 2000).

In vertebrates, although neurons synthesize the absolute minimum of required cholesterol, glial production and release of lipoproteins supply neuronal demand during development and in adulthood (Mauch et al., 2001). In particular, apolipoprotein E (APOE) is synthesized primarily by astrocytes and glial cells (Boyles et al., 1985; Pfrieger & Ungerer, 2011). Glia-derived cholesterol stimulates synapse formation and synaptic efficacy (Pfrieger, 2003a, 2003b). In the presynaptic plasma membrane, cholesterol-rich lipid rafts are necessary for SNARE-dependent exocytosis of vesicles with high cholesterol content. At the postsynaptic level, such rafts organize the disposition of receptors, protein scaffolds, and signaling cascades (Pfrieger, 2003a, 2003b). Importantly, cholesterol removal from neuronal cultures impairs exocytosis of synaptic vesicles (Linetti et al., 2010), synaptic transmission (Goritz et al., 2005), and neuronal viability (Michikawa & Yanagisawa, 1999). In addition, cholesterol induces clustering of AMPA receptors and hinders NMDA-induced long-term potentiation in the hippocampus (Frank et al., 2008; Martín et al., 2014).

Two consensus motifs with predictive value for cholesterol interaction with proteins have been defined through in silico methods (Di Scala et al., 2017), CRAC and CARC (Baier et al., 2011; Li & Papadopoulos, 1998). The non-covalent binding of cholesterol to such motifs has been the focus of several recent studies. For example, cholesterol modulates docking of NMDA receptors into lipid rafts (Korinek et al., 2015) and regulates the function of vanilloid receptors TRPV1, a member of the TRP family (Jansson et al., 2013), thus interfering in synaptic plasticity. Increased cholesterol concentration enhances the plasticity and flexibility of 5HT1a dimers and adrenergic receptors (Prasanna et al., 2014, 2016). Given the opposed dispositions of CARC and CRAC motifs, it is possible to assume the co-existence of both in the same transmembrane domain and their potential interaction with two cholesterol molecules in a tail-to-tail configuration (Di Scala et al., 2017). However, none of the analyzed TMR of RTK family members in the present study displayed co-existing CARC and CRAC motifs.

Interestingly, we observed the occurrence of CARC motifs only in the zebrafish, mouse, and human RTK family. Moreover, only three vertebrate RTKs: NTRK2 (TRKB), ROR2 and RYK, were found to possess a CARC domain within the TMR. ROR2 is a member of the ROR family, closely related to the TRK family, and plays a distinct role in bone morphogenesis, through a signaling cascade not yet fully described but engaging 14–3-3β scaffolding proteins (Liu et al., 2007). RYK receptor is an atypical member of the RTK family, as it lacks tyrosine kinase activity while containing the related kinase characteristic of the family (Hovens et al., 1992). In mammalian cells, RYK serves as a co-receptor with Frizzled for Wnt ligands mediating neurite outgrowth (Lu et al., 2004).

The insights from the present study can serve as a primary step to experimentally test the impact of mutations in CRAC/CARC motifs in the TMR of the RTK family. However, we are limited by only considering the role of CRAC/CARC motifs in the TMR of RTKs. Given the promiscuous properties of these motifs, it is plausible to assume multiple false-positive CRAC/CARCs in proteins, making data mining and putative in silico or in vitro analysis difficult to perform. Therefore, more studies focused on refining the algorithms for detecting cholesterol-binding motifs are necessary.

TRKB plays a crucial role in several aspects of neuronal plasticity (Park & Poo, 2013). The activation of this receptor is associated with the reopening of the visual critical period (Maya Vetencourt et al., 2008) and the formation, retention, and recall of memory (Bekinschtein et al., 2014; Karpova et al., 2011). TRKB.TMR is highly conserved among vertebrates, similar to full-length TRKB. Although correlated, the identity of full-length TRKB and TRKB.TMR are not comparable. Given the large difference in the number of residues between these two sequences, each residue change in the TMR exerts a higher impact than on full-length TRKB in the overall identity between the species analyzed. However, the TRKB.TMR CARC sequence from chicken differs in the juxtamembrane residues from the other species compared here (Table 2). The following two scenarios are plausible. The role of R/K (charged, basic residues) is fulfilled by glutamate (E), which is also charged at pH 7, although negatively; or by asparagine (N), which is not charged but carries a basic amino group. Additionally, for the second possibility, it is also necessary to relax the proposed "5-residue rule" between the Y and the juxtamembrane residue (Fantini et al., 2019) since N is located 6 residues apart from the central Y. Nonetheless, our MD simulations indicate that cholesterol interacts with TRKB mainly through the CARC central Y residue in this receptor, as the interaction values between the C-alpha atom in Y433 residue are 10-fold higher than those between cholesterol and the R427, suggesting that chicken TRKB might still be able to interact with cholesterol. Moreover, the cholesterol interaction with TRKB, measured by microscale thermophoresis, is completely lost

in the single mutant Y433F, reinforcing the central role for Y in this interaction (Casarotto et al., 2021).

TRKB is found in lipid rafts only upon activation by BDNF (Suzuki et al., 2004). Interestingly, when cholesterol is sequestered, TRKB translocation to lipid rafts is impaired, and BDNF-dependent activation of TRKB is prevented (Suzuki et al., 2004). However, reduction in cholesterol in hippocampal cultures is associated with increased baseline activity of TRKB (Martin et al., 2008). These opposite outcomes might be due to a differential modulation exerted by cholesterol, depending on the activity of TRKB receptor (basal vs. BDNF-stimulated), cell type or origin, and stage of differentiation. Another explanation is that cholesterol affects TRKB activity in a bell-shaped manner, where higher and lower cholesterol concentrations impede instead of promoting TRKB phosphorylation, as observed here. In fact, the decrease of cholesterol levels by beta-cyclodextrin was found to differentially modulate neurite growth of hippocampal and cortical cultured neurons (Ko et al., 2005). In hippocampal cells, the decrease of cholesterol levels induced an increase in neurite length and number, while no effect was observed in cortical cells. Interestingly, cultures of hippocampal cells revealed higher levels of cholesterol than the cortical counterparts (Ko et al., 2005).

We propose that TRKB has evolved to become a "sensor" of cholesterol levels in the cell membrane via CARC. Thus, TRKB would trigger synaptic maturation or neurite growth, only if the cholesterol levels are optimal for such changes, that is cholesterol concentrations must be within a 'Goldilocks' zone. In fact, our previous data indicate that cholesterol modulates BDNF-induced TRKB activation in a bell-shaped fashion (Casarotto et al., 2021). Under low amounts of supplemented cholesterol, the activation of TRKB by BDNF is facilitated, while at higher concentrations (around 50 μM), this increment is lost, and even compromised under higher amounts of cholesterol (around 100 μM). Inhibiting cholesterol synthesis also compromised BDNF-induced TRKB activation (Suzuki et al., 2004). In line with this evidence, we observed here the same pattern over BDNF binding to TRKB. TRKB dimerization is heavily influenced by cholesterol, mainly through changes in the membrane thickness, which changes the orientation of TRKB dimers between competent and incompetent conformations for signaling (Casarotto et al., 2021), and the present data provide additional evidence that such changes may also influence BDNF interaction with TRKB. Taken together, our data suggest that cholesterol, by modulating the TRKB dimer orientation, changes the exposure of binding sites for BDNF in TRKB, which in turn reflects changes in signaling.

AUTHOR CONTRIBUTIONS AND CONFLICT OF INTEREST

CC, MF, PC, CB designed and conducted the data mining and binding experiments. MG, GE, and TR designed and conducted the molecular dynamics experiments. CC, MG, GE, PC, CB, and MF wrote the first draft of the manuscript, edited by TR, IV, and EC. EC received lecture fees from Janssen-Cilag. All other authors declare no competing interests.

6 | DATA SHARING

The data used in the present study are available in FigShare under CC-BY license (https://doi.org/10.6084/m9.figsh are.7935980).

PEER REVIEW
The peer review history for this article is available at https://publons.com/publon/10.1111/ejn.15218.

ORCID
Cecilia Cannarozzo [ID] https://orcid.org/0000-0002-5676-3619
Senem Merve Fred [ID] https://orcid.org/0000-0003-1992-5014
Mykhailo Girych [ID] https://orcid.org/0000-0002-6046-518X
Caroline Biojone [ID] https://orcid.org/0000-0002-9674-4930
Giray Enkavi [ID] https://orcid.org/0000-0001-5033-8649
Tomasz Róg [ID] https://orcid.org/0000-0001-6765-7013
Ilpo Vattulainen [ID] https://orcid.org/0000-0001-7408-3214
Plinio C Casarotto [ID] https://orcid.org/0000-0002-1090-4631
Eero Castrén [ID] https://orcid.org/0000-0002-1402-2791

REFERENCES
Abraham, M. J., Murtola, T., Schulz, R., Páll, S., Smith, J. C., Hess, B., & Lindahl, E. (2015). GROMACS: High performance molecular simulations through multi-level parallelism from laptops to supercomputers. *SoftwareX*, *1–2*, 19–25. https://doi.org/10.1016/j.softx.2015.06.001

Arnarez, C., Uusitalo, J. J., Masman, M. F., Ingólfsson, H. I., de Jong, D. H., Melo, M. N., Periole, X., de Vries, A. H., & Marrink, S. J. (2015). Dry Martini, a coarse-grained force field for lipid membrane simulations with implicit solvent. *Journal of Chemical Theory and Computation*, *11*, 260–275.

Baeza-Raja, B., Sachs, B. D., Li, P., Christian, F., Vagena, E., Davalos, D., Le Moan, N., Ryu, J. K., Sikorski, S. L., Chan, J. P., Scadeng, M., Taylor, S. S., Houslay, M. D., Baillie, G. S., Saltiel, A. R., Olefsky, J. M., & Akassoglou, K. (2016). p75 neurotrophin receptor regulates energy balance in obesity. *Cell Reports*, *14*, 255–268.

Baier, C. J., Fantini, J., & Barrantes, F. J. (2011). Disclosure of cholesterol recognition motifs in transmembrane domains of the human nicotinic acetylcholine receptor. *Scientific Reports*, *1*, 69.

Bekinschtein, P., Cammarota, M., & Medina, J. H. (2014). BDNF and memory processing. *Neuropharmacology*, *76*, 677–683. https://doi.org/10.1016/j.neuropharm.2013.04.024

Boyles, J. K., Pitas, R. E., Wilson, E., Mahley, R. W., & Taylor, J. M. (1985). Apolipoprotein E associated with astrocytic glia of the central nervous system and with nonmyelinating glia of the peripheral nervous system. *Journal of Clinical Investigation*, *76*, 1501–1513. https://doi.org/10.1172/JCI112130

Bussi, G., Donadio, D., & Parrinello, M. (2007). Canonical sampling through velocity rescaling. *The Journal of Chemical Physics*, *126*, 014101.

Casarotto, P. C., Girych, M., Fred, S. M., Kovaleva, V., Moliner, R., Enkavi, G., Biojone, C., Cannarozzo, C., Sahu, M. P., Kaurinkoski, K., Brunello, C. A., Steinzeig, A., Winkel, F., Patil, S., Vestring, S., Serchov, T., Diniz, C. R. A. F., Laukkanen, L., Cardon, I., … Castrén, E. (2021). Antidepressant drugs act by directly binding to TRKB neurotrophin receptors. *Cell*, *184*, 1299–1313.e19.

Das, I., Krzyzosiak, A., Schneider, K., Wrabetz, L., D'Antonio, M., Barry, N., Sigurdardottir, A., & Bertolotti, A. (2015). Preventing proteostasis diseases by selective inhibition of a phosphatase regulatory subunit. *Science*, *348*, 239–242. https://doi.org/10.1126/science.aaa4484

de Chaves, E. I., Rusiñol, A. E., Vance, D. E., Campenot, R. B., & Vance, J. E. (1997). Role of lipoproteins in the delivery of lipids to axons during axonal regeneration. *Journal of Biological Chemistry*, *272*, 30766–30773.

de Jong, D. H., Baoukina, S., Ingólfsson, H. I., & Marrink, S. J. (2016). Martini straight: Boosting performance using a shorter cutoff and GPUs. *Computer Physics Communications*, *199*, 1–7.

de Jong, D. H., Singh, G., Bennett, W. F. D., Arnarez, C., Wassenaar, T. A., Schäfer, L. V., Periole, X., Tieleman, D. P., & Marrink, S. J. (2013). Improved parameters for the martini coarse-grained protein force field. *Journal of Chemical Theory and Computation*, *9*, 687–697.

Dekkers, M. P. J., Nikoletopoulou, V., & Barde, Y.-A. (2013). Cell biology in neuroscience: Death of developing neurons: New insights and implications for connectivity. *Journal of Cell Biology*, *203*, 385–393.

Di Scala, C., Baier, C. J., Evans, L. S., Williamson, P. T. F., Fantini, J., & Barrantes, F. J. (2017). Chapter one - relevance of CARC and CRAC cholesterol-recognition motifs in the nicotinic acetylcholine receptor and other membrane-bound receptors. In I. Levitan (Ed.), *Current topics in membranes, sterol regulation of ion channels* (pp. 3–23): Cambridge, MA: Academic Press.

Dietschy, J. M., & Turley, S. D. (2004). Thematic review series: Brain Lipids. Cholesterol metabolism in the central nervous system during early development and in the mature animal. *Journal of Lipid Research*, *45*, 1375–1397. https://doi.org/10.1194/jlr.R400004-JLR200

Elkins, M. R., Sergeyev, I. V., & Hong, M. (2018). Determining cholesterol binding to membrane proteins by cholesterol 13c labeling in yeast and dynamic nuclear polarization NMR. *Journal of the American Chemical Society*, *140*, 15437–15449.

Epand, R. M. (2006). Cholesterol and the interaction of proteins with membrane domains. *Progress in Lipid Research*, *45*, 279–294.

Fantini, J., & Barrantes, F. J. (2013). How cholesterol interacts with membrane proteins: An exploration of cholesterol-binding sites including CRAC, CARC, and tilted domains. *Frontiers in Physiology*, *4*, 31. https://doi.org/10.3389/fphys.2013.00031

Fantini, J., Di Scala, C., Evans, L. S., Williamson, P. T. F., & Barrantes, F. J. (2016). A mirror code for protein-cholesterol interactions in the two leaflets of biological membranes. *Scientific Reports*, *6*, 21907.

Fantini, J., Epand, R. M., & Barrantes, F. J. (2019). Cholesterol-recognition motifs in membrane proteins. *Advances in Experimental Medicine and Biology*, *1135*, 3–25.

Frank, C., Rufini, S., Tancredi, V., Forcina, R., Grossi, D., & D'Arcangelo, G. (2008). Cholesterol depletion inhibits synaptic transmission and synaptic plasticity in rat hippocampus. *Experimental Neurology*, *212*, 407–414.

Goritz, C., Mauch, D. H., & Pfrieger, F. W. (2005). Multiple mechanisms mediate cholesterol-induced synaptogenesis in a CNS neuron. *Molecular and Cellular Neurosciences*, *29*, 190–201.

Hanson, M. A., Cherezov, V., Griffith, M. T., Roth, C. B., Jaakola, V.-P., Chien, E. Y. T., Velasquez, J., Kuhn, P., & Stevens, R. C. (2008). A specific cholesterol binding site is established by the 2.8 A structure of the human beta2-adrenergic receptor. *Structure*, *16*, 897–905.

Harris, J. S., Epps, D. E., Davio, S. R., & Kézdy, F. J. (1995). Evidence for transbilayer, tail-to-tail cholesterol dimers in dipalmitoylglycerophosphocholine liposomes. *Biochemistry*, *34*, 3851–3857. https://doi.org/10.1021/bi00011a043

Hovens, C. M., Stacker, S. A., Andres, A. C., Harpur, A. G., Ziemiecki, A., & Wilks, A. F. (1992). RYK, a receptor tyrosine kinase-related molecule with unusual kinase domain motifs. *Proceedings of the National Academy of Sciences of the United States of America*, *89*, 11818–11822.

Hsu, P.-C., Bruininks, B. M. H., Jefferies, D., Telles, C., de Souza, P., Lee, J., Patel, D. S., Marrink, S. J., Qi, Y., Khalid, S., & Im, W. (2017). CHARMM-GUI Martini Maker for modeling and simulation of complex bacterial membranes with lipopolysaccharides. *Journal of Computational Chemistry*, *38*, 2354–2363.

Huang, E. J., & Reichardt, L. F. (2001). Neurotrophins: Roles in neuronal development and function. *Annual Review of Neuroscience*, *24*, 677–736.

Hunte, C. (2005). Specific protein-lipid interactions in membrane proteins. *Biochemical Society Transactions*, *33*, 938–942.

Jamin, N., Neumann, J.-M., Ostuni, M. A., Vu, T. K. N., Yao, Z.-X., Murail, S., Robert, J.-C., Giatzakis, C., Papadopoulos, V., & Lacapère, J.-J. (2005). Characterization of the cholesterol recognition amino acid consensus sequence of the peripheral-type benzodiazepine receptor. *Molecular Endocrinology*, *19*, 588–594.

Jansson, E. T., Trkulja, C. L., Ahemaiti, A., Millingen, M., Jeffries, G. D., Jardemark, K., & Orwar, O. (2013). Effect of cholesterol depletion on the pore dilation of TRPV1. *Molecular Pain*, *9*, 1.

Jeong, J., & McMahon, A. P. (2002). Cholesterol modification of Hedgehog family proteins. *Journal of Clinical Investigation*, *110*, 591–596.

Karpova, N. N., Pickenhagen, A., Lindholm, J., Tiraboschi, E., Kulesskaya, N., Agústsdóttir, A., Antila, H., Popova, D., Akamine, Y., Bahi, A., Sullivan, R., Hen, R., Drew, L. J., & Castrén, E. (2011). Fear erasure in mice requires synergy between antidepressant drugs and extinction training. *Science*, *334*, 1731–1734. https://doi.org/10.1126/science.1214592

Ko, M., Zou, K., Minagawa, H., Yu, W., Gong, J.-S., Yanagisawa, K., & Michikawa, M. (2005). Cholesterol-mediated neurite outgrowth is differently regulated between cortical and hippocampal neurons. *Journal of Biological Chemistry*, *280*, 42759–42765.

Korinek, M., Vyklicky, V., Borovska, J., Lichnerova, K., Kaniakova, M., Krausova, B., Krusek, J., Balik, A., Smejkalova, T., Horak, M., & Vyklicky, L. (2015). Cholesterol modulates open probability and desensitization of NMDA receptors. *Journal of Physiology*, *593*, 2279–2293.

Kurzchalia, T. V., & Ward, S. (2003). Why do worms need cholesterol? *Nature Cell Biology*, *5*, 684–688.

Landrum, M. J., Lee, J. M., Benson, M., Brown, G. R., Chao, C., Chitipiralla, S., Gu, B., Hart, J., Hoffman, D., Jang, W., Karapetyan, K., Katz, K., Liu, C., Maddipatla, Z., Malheiro, A., McDaniel, K., Ovetsky, M., Riley, G., Zhou, G., … Maglott, D. R. (2018). ClinVar: Improving access to variant interpretations and supporting evidence. *Nucleic Acids Research*, *46*, D1062–D1067. https://doi.org/10.1093/nar/gkx1153

Lang, T., Bruns, D., Wenzel, D., Riedel, D., Holroyd, P., Thiele, C., & Jahn, R. (2001). SNAREs are concentrated in cholesterol-dependent clusters that define docking and fusion sites for exocytosis. *EMBO Journal*, *20*, 2202–2213.

Lee, A. G. (2004). How lipids affect the activities of integral membrane proteins. *Biochimica Et Biophysica Acta*, *1666*, 62–87.

Li, H., & Papadopoulos, V. (1998). Peripheral-type benzodiazepine receptor function in cholesterol transport. Identification of a putative cholesterol recognition/interaction amino acid sequence and consensus pattern. *Endocrinology*, *139*, 4991–4997.

Linetti, A., Fratangeli, A., Taverna, E., Valnegri, P., Francolini, M., Cappello, V., Matteoli, M., Passafaro, M., & Rosa, P. (2010). Cholesterol reduction impairs exocytosis of synaptic vesicles. *Journal of Cell Science*, *123*, 595–605.

Liu, J.-P., Tang, Y., Zhou, S., Toh, B. H., McLean, C., & Li, H. (2010). Cholesterol involvement in the pathogenesis of neurodegenerative diseases. *Molecular and Cellular Neurosciences*, *43*, 33–42.

Liu, Y., Ross, J. F., Bodine, P. V. N., & Billiard, J. (2007). Homodimerization of Ror2 tyrosine kinase receptor induces 14-3-3(beta) phosphorylation and promotes osteoblast differentiation and bone formation. *Molecular Endocrinology*, *21*, 3050–3061.

Lomize, A. L., Hage, J. M., & Pogozheva, I. D. (2018). Membranome 2.0: Database for proteome-wide profiling of bitopic proteins and their dimers. *Bioinformatics*, *34*, 1061–1062. https://doi.org/10.1093/bioinformatics/btx720

Lu, W., Yamamoto, V., Ortega, B., & Baltimore, D. (2004). Mammalian Ryk is a Wnt coreceptor required for stimulation of neurite outgrowth. *Cell*, *119*, 97–108. https://doi.org/10.1016/j.cell.2004.09.019

Maguire, P. A., & Druse, M. J. (1989). The influence of cholesterol on synaptic fluidity, dopamine D1 binding and dopamine-stimulated adenylate cyclase. *Brain Research Bulletin*, *23*, 69–74.

Mann, R. K., & Beachy, P. A. (2000). Cholesterol modification of proteins. *Biochimica Et Biophysica Acta*, *1529*, 188–202.

Martin, M. G., Ahmed, T., Korovaichuk, A., Venero, C., Menchón, S. A., Salas, I., Munck, S., Herreras, O., Balschun, D., & Dotti, C. G. (2014). Constitutive hippocampal cholesterol loss underlies poor cognition in old rodents. *EMBO Molecular Medicine*, *6*, 902–917.

Martin, M. G., Perga, S., Trovò, L., Rasola, A., Holm, P., Rantamäki, T., Harkany, T., Castrén, E., Chiara, F., & Dotti, C. G. (2008). Cholesterol loss enhances TrkB signaling in hippocampal neurons aging in vitro. *Molecular Biology of the Cell*, *19*, 2101–2112.

Martín, M. G., Pfrieger, F., & Dotti, C. G. (2014). Cholesterol in brain disease: Sometimes determinant and frequently implicated. *EMBO Reports*, *15*, 1036–1052. https://doi.org/10.15252/embr.201439225

Mauch, D. H., Nägler, K., Schumacher, S., Göritz, C., Müller, E. C., Otto, A., & Pfrieger, F. W. (2001). CNS synaptogenesis promoted by glia-derived cholesterol. *Science*, *294*, 1354–1357. https://doi.org/10.1126/science.294.5545.1354

Maya Vetencourt, J. F., Sale, A., Viegi, A., Baroncelli, L., De Pasquale, R., O'Leary, O. F., Castrén, E., & Maffei, L. (2008). The antidepressant fluoxetine restores plasticity in the adult visual cortex. *Science*, *320*, 385–388. https://doi.org/10.1126/science.1150516

Michikawa, M., & Yanagisawa, K. (1999). Inhibition of cholesterol production but not of nonsterol isoprenoid products induces neuronal cell death. *Journal of Neurochemistry*, *72*, 2278–2285.

Mottaz, A., David, F. P. A., Veuthey, A.-L., & Yip, Y. L. (2010). Easy retrieval of single amino-acid polymorphisms and phenotype information using SwissVar. *Bioinformatics*, *26*, 851–852. https://doi.org/10.1093/bioinformatics/btq028

Nieweg, K., Schaller, H., & Pfrieger, F. W. (2009). Marked differences in cholesterol synthesis between neurons and glial cells from postnatal rats. *Journal of Neurochemistry*, *109*, 125–134.

Nikoletopoulou, V., Lickert, H., Frade, J. M., Rencurel, C., Giallonardo, P., Zhang, L., Bibel, M., & Barde, Y.-A. (2010). Neurotrophin receptors TrkA and TrkC cause neuronal death whereas TrkB does not. *Nature*, *467*, 59–63. https://doi.org/10.1038/nature09336

Niwa, Y. S., & Niwa, R. (2014). Neural control of steroid hormone biosynthesis during development in the fruit fly Drosophila melanogaster. *Genes & Genetic Systems*, *89*, 27–34.

Páll, S., & Hess, B. (2013). A flexible algorithm for calculating pair interactions on SIMD architectures. *Computer Physics Communications*, *184*(12), 2641–2650. https://doi.org/10.1016/j.cpc.2013.06.003

Park, H., & Poo, M.-M. (2013). Neurotrophin regulation of neural circuit development and function. *Nature Reviews Neuroscience*, *14*, 7–23.

Parrinello, M., & Rahman, A. (1981). Polymorphic transitions in single crystals: A new molecular dynamics method. *Journal of Applied Physics*, *52*, 7182.

Pereira, D. B., & Chao, M. V. (2007). The tyrosine kinase Fyn determines the localization of TrkB receptors in lipid rafts. *Journal of Neuroscience*, *27*, 4859–4869.

Peters, M., Katz, B., Lev, S., Zaguri, R., Gutorov, R., & Minke, B. (2017). Depletion of membrane cholesterol suppresses drosophila transient receptor potential-like (TRPL) channel activity. *Current Topics in Membranes*, *80*, 233–254.

Pfrieger, F. W. (2003a). Role of cholesterol in synapse formation and function. *Biochimica Et Biophysica Acta*, *1610*, 271–280. https://doi.org/10.1016/S0005-2736(03)00024-5

Pfrieger, F. W. (2003b). Outsourcing in the brain: Do neurons depend on cholesterol delivery by astrocytes? *BioEssays*, *25*, 72–78. https://doi.org/10.1002/bies.10195

Pfrieger, F. W., & Ungerer, N. (2011). Cholesterol metabolism in neurons and astrocytes. *Progress in Lipid Research*, *50*, 357–371.

Prasanna, X., Chattopadhyay, A., & Sengupta, D. (2014). Cholesterol modulates the dimer interface of the β_2-adrenergic receptor via cholesterol occupancy sites. *Biophysical Journal*, *106*, 1290–1300.

Prasanna, X., Sengupta, D., & Chattopadhyay, A. (2016). Cholesterol-dependent Conformational Plasticity in GPCR Dimers. *Scientific Reports*, *6*, 31858.

Quan, G., Xie, C., Dietschy, J. M., & Turley, S. D. (2003). Ontogenesis and regulation of cholesterol metabolism in the central nervous system of the mouse. *Brain Research. Developmental Brain Research*, *146*, 87–98.

Rukmini, R., Rawat, S. S., Biswas, S. C., & Chattopadhyay, A. (2001). Cholesterol organization in membranes at low concentrations: Effects

of curvature stress and membrane thickness. *Biophysical Journal*, *81*, 2122–2134. https://doi.org/10.1016/S0006-3495(01)75860-2

Saito, K., Dubreuil, V., Arai, Y., Wilsch-Bräuninger, M., Schwudke, D., Saher, G., Miyata, T., Breier, G., Thiele, C., Shevchenko, A., Nave, K.-A., & Huttner, W. B. (2009). Ablation of cholesterol biosynthesis in neural stem cells increases their VEGF expression and angiogenesis but causes neuron apoptosis. *Proceedings of the National Academy of Sciences of the United States of America*, *106*, 8350–8355.

Suzuki, S., Kiyosue, K., Hazama, S., Ogura, A., Kashihara, M., Hara, T., Koshimizu, H., & Kojima, M. (2007). Brain-derived neurotrophic factor regulates cholesterol metabolism for synapse development. *Journal of Neuroscience*, *27*, 6417–6427. https://doi.org/10.1523/JNEUROSCI.0690-07.2007

Suzuki, S., Numakawa, T., Shimazu, K., Koshimizu, H., Hara, T., Hatanaka, H., Mei, L., Lu, B., & Kojima, M. (2004). BDNF-induced recruitment of TrkB receptor into neuronal lipid rafts: Roles in synaptic modulation. *Journal of Cell Biology*, *167*, 1205–1215.

Tate, J. G., Bamford, S., Jubb, H. C., Sondka, Z., Beare, D. M., Bindal, N., Boutselakis, H., Cole, C. G., Creatore, C., Dawson, E., Fish, P., Harsha, B., Hathaway, C., Jupe, S. C., Kok, C. Y., Noble, K., Ponting, L., Ramshaw, C. C., Rye, C. E., … Forbes, S. A. (2019). COSMIC: The catalogue of somatic mutations in cancer. *Nucleic Acids Research*, *47*, D941–D947. https://doi.org/10.1093/nar/gky1015

The UniProt Consortium (2017). UniProt: The universal protein knowledgebase. *Nucleic Acids Research*, *45*, D158–D169.

Waterhouse, A. M., Procter, J. B., Martin, D. M. A., Clamp, M., & Barton, G. J. (2009). Jalview Version 2–a multiple sequence alignment editor and analysis workbench. *Bioinformatics*, *25*, 1189–1191. https://doi.org/10.1093/bioinformatics/btp033

Wendler, F., Franch-Marro, X., & Vincent, J.-P. (2006). How does cholesterol affect the way Hedgehog works? *Development*, *133*, 3055–3061. https://doi.org/10.1242/dev.02472

Zonta, B., & Minichiello, L. (2013). Synaptic membrane rafts: Traffic lights for local neurotrophin signaling? *Frontiers in Synaptic Neuroscience*, *5*, 9.

SUPPORTING INFORMATION

Additional supporting information may be found online in the Supporting Information section.